bioRxiv (2024)
doi:10.1101/2021.11.27.470201
a Malthusian Relativity paper

$\iota^{**}=7/3\psi$
mrLife.org

Birds and mammals have natural selection regulated population dynamics

Lars Witting
Greenland Institute of Natural Resources, Box 570, DK-3900 Nuuk, Greenland. lawi@natur.gl

Abstract Ecological dynamics is increasingly explained by eco-evolutionary processes, with this study analysing natural selection effects on the population dynamics of birds and mammals. Fitting single-species population dynamic models to 3,369 and 483 timeseries for 900 species of birds and 208 mammals, I find selection-based population dynamic models to be 780 (se:1.3) to 150,000 (se:2) times more probable than models with no selection. Selection is essential in 79% to 92% of AIC selected models, explaining 80% of the population dynamics variance, with median selection regulation being 1.2 (se:0.11) times stronger than density regulation. The estimated dynamics is cyclic with median damping ratios of 0.12 (se:0.0071) and 0.062 (se:0.021) for birds and mammals, and median population periods of 8.3 (se:0.99) and 7.2 (se:0.85) generations for stable cycles with damping ratios around zero. These results resolve several enigmas of population cycles, highlighting the importance of integrating natural selection into population dynamics.

Keywords: Density dependence, eco-evolutionary dynamics, natural selection, population dynamics, population regulation, timeseries

1 Introduction

Population regulation shapes the dynamics of natural populations, but traditional single-species population regulation theory fails to explain even simple population dynamic trajectories. Take for example a population that declines gradually until the decline stops and the population begins to increase. This is an often-observed growth pattern, but density dependent competition does not explain it. Density regulated populations will only increase, or decline, towards carrying capacity showing no change in the direction of growth (over-compensation from strong density regulation does not explain a gradual change in the direction of growth).

For the past century or so, variation in environmental drivers provided the conceptual solution to the lack of fit between single-species population regulation theory and data. These drivers may be density dependent or independent, including environmental fluctuations, climatic change, predators, and prey. With the dynamics of natural populations correlating with environmental factors (e.g. Elton 1924; Koenig 2002; Jenkins et al. 2022), evidence suggests that deviations from density regulated growth follow from external perturbations. The vast majority of the available timeseries of abundance estimates, however, have no associated data to confirm the extrinsic hypothesis. It is therefore often of limited practical use and is perhaps more often a convenient *ad hoc* explanation for the lack of fit between single-species theory and data.

Delayed density regulated models provide a practical solution, generating "single-species" models that "explain" much of the observed dynamics (e.g. Turchin and Taylor 1992; Hörnfeldt 1994; Hansen et al. 1999). But delayed density regulated studies turn the blind eye to the real problem: the absence of identified but necessary population dynamic interactions. By explicitly not incorporating biological mechanisms for the delayed regulation, delayed density regulation fails to explain the observed dynamics from population biological mechanisms.

If we concentrate on studies with a population mechanistic focus, explanations have advanced by spatial synchrony (Ranta et al. 1995; Liebhold et al. 2004), stochasticity (Kaitala et al. 1996; McKane and Newman 2005), environmental oscillations (Post and Forchhammer 2002; Taylor et al. 2013), maternal effects (Ginzburg 1998), demographic details (Murdoch et al. 2002; McCauley et al. 2008), and higher-dimensional interactions (Tyson et al. 2010; Liu et al. 2013; Martínez-Padilla et al. 2014). But several enduring enigmas remain unsolved by this broader population dynamic theory (Myers 2018; Oli 2019; Andreassen et al. 2021).

These issues include the link between population cycles and trophic interactions, a theoretical dependence that seems not to apply to natural populations. One example is the isolated *Daphnia*-algae system analysed by Murdoch and McCauley (1985), where *Daphnia* were found to cycle with a relatively fixed period independently of the presence versus absence of a cycle in algae. A similar paradox includes snowshoe hares that cycle

in the absence of lynx (Keith 1963), and the absence of a firm predator-prey interaction for one of best documented cycles in forest insects (Berryman 1996).

Another problem is the widespread presence of life history changes in phase with population dynamic cycles, changes that do not follow from density regulation, nor from interactions between predators and prey. Where predation affects survival, "most, if not all, cyclic rodent populations are characterised by phase related changes in body mass, social behaviour, ... and reproductive rates" (Oli 2019). These life history cycles are a real paradox, as reproduction remains low across the low phase of population cycles, where it should be high due to relaxed density regulation (Myers 2018).

Other lingering problems include that no experimental manipulation of predators and resources "has succeeded in stopping rodent population cycles anywhere" (Oli 2019), and "how can low amplitude cycles persist if high densities are required for the build-up of predators, parasitoids, pathogens or detrimental conditions" (Myers 2018).

These issues do not question population dynamics influenced by external factors, but they hint at a population dynamic theory that lacks essential population dynamic mechanisms. In my search for such a mechanism, I analyse the way populations regulate their own growth when other things are equal. I take the parsimonious view that to explain the growth of natural populations we need first of all to understand how they regulate their own growth.

A focus on internal population regulation is important because it is this most basic population regulation that sets the stage of our population dynamic investigations. It is e.g. the monotonic growth of density regulated populations that lead many biologists towards external explanations for the observed population dynamics. But internal population regulation is not restricted to density regulation, as intra-specific natural selection is also regulating the growth and abundance of populations (Witting 1997, 2000). From an eco-evolutionary point of view, the lack of fit between traditional single-species population regulation theory and data is not surprising, as it assumes that natural selection does not affect population dynamics. Hence, I analyse 3,852 population dynamic timeseries in an attempt to estimate if natural selection is the missing population regulation component that will make our single species model work as a first approximation to the population dynamics of birds and mammals.

1.1 On natural selection regulation

With the Malthusian parameter r being the natural selection fitness of the individual (Fisher 1930), and the average Malthusian parameter being the exponential growth rate of the population, the population dynamic growth rate is the trait that is exposed to the strongest natural selection, capturing the natural selection variation in other traits. It is therefore not surprising if natural selection affects population dynamic growth.

A first attempt to include evolution in population dynamics was based on self-regulation by group-selection (Wynne-Edwards 1959, 1986), relating to the Chitty (1960) hypothesis. This approach, however, was criticised for unrealistic assumptions (Stenseth 1981). I use a different game theoretical selection that was integrated into population dynamic theory about 25 years ago, focussing on individual selection by intra-specific density dependent interactive competition (Witting 1997, 2000). These interactions generate a population dynamic feedback selection, with the resulting models including regulation from both density dependent competition and density frequency dependent natural selection.

This regulation by natural selection accelerates population dynamic growth at abundancies below the naturally selected population dynamic equilibrium, and decelerates growth above, generating cyclic dynamics that converge on hyperexponential growth at zero abundance (Witting 2000). The predicted population cycles are phase-forgetting damped in most cases, with amplitudes and cyclic regularities that dependent on the magnitudes and frequencies of external perturbations. This dynamics successfully replicates the population cycles of forest insects (Witting 1997, 2000) and the delayed recovery of large whales following commercial exploitation in past centuries (Witting 2013).

Where density regulation suppresses population dynamic growth by density dependent competition, selection regulation accelerates and decelerates population growth dependent upon the distribution of differences in the Malthusian parameter across the individuals in the population. This intra-population growth differentiation is under active feedback selection from density dependent interactive competition (Witting 2000), and it is selected as a balance between the quality-quantity trade-off and the interactive quality that individuals use to monopolise resources during interactive competition. Where the quality-quantity trade-off selects for a decline in quality and increased reproduction, interactive competition selects for increased quality and decreased reproduction, with the two selection forces balanced

against one another at the naturally selected population dynamic equilibrium.

The distinction between density regulation and selection regulation is clear on theoretical grounds. But to play a real role the regulating force must change across the densities experienced by natural populations. This is expected for selection regulation by the differentiated selection for increased and decreased growth below and above the population dynamic equilibrium. The evolutionary scope of this naturally selected population dynamic equilibrium consolidates this expectation, as the equilibrium is also a selection attractor that explains the evolutionary existence of multicellular animals with non-negligible body masses, sexual reproduction, and inter-specific body mass allometries (Witting 2002, 2017). If the feedback attractor did not balance the two opposing forces of selection, we should see either a selection collapse towards asexual self-replicating cells, or intra-specific naturally selected arms races that would cause the extinction of populations.

Selection regulation is furthermore supported by empirical studies on population dynamic responses to natural selection. This evidence includes *i*) a two-generation cycle in the abundance and competitive quality of side-blotched lizard (*Uta stansburiana*) in response to selection by density dependent interactive competition (Sinervo et al. 2000), *ii*) a selection acceleration of the population dynamic growth rate by up to 40% over few generations (Turcotte et al. 2011), *iii*) the selection of faster-spreading Covid-19 variants generating hyperexponential growth (Halley et al. 2021; Pavithran and Sujith 2022), and *iv*) an increasing number of eco-evolutionary studies that document evolutionary dynamics on ecological timescales (e.g. Thompson 1998; Saccheri and Hanski 2006; Coulson et al. 2011; Brunner et al. 2019), including *v*) evolutionary rescue where selection accelerates the growth rate turning a population decline into increase (e.g. Gomulkiewicz and Holt 1995; Agashe 2009; Bell and Gonzalez 2009).

Additional evidence comes from the otherwise unresolved issues with population dynamic cycles, where the selected change in population growth follows from selected changes in the life history. This prediction includes selection for lower reproduction, larger body masses, increased competitive behaviour like aggression, kin groups, and more interacting males at high population densities, and selection for the opposite at low densities (Witting 1997, 2000). Being widespread in natural populations with cyclic dynamics, these phase related life history changes provide plenty of literature evidence in favour of selection regulation. This includes e.g. a body mass cycle in the *Daphnia* experiments of Murdoch and McCauley (1985), with larger individuals occurring mainly in the late peak phase of a cycle, and smaller individuals mainly in the early increasing phase (Witting 2000). Similar changes in body mass are widespread in voles and lemmings with cyclic dynamics (e.g. Boonstra and Krebs 1979; Lidicker and Ostfeld 1991; Norrdahl and Korpimäki 2002), and they have been observed in snowshoe hare (Hodges et al. 1999) and cyclic forest insects (Myers 1990; Simchuk et al. 1999).

Naumov et al. (1969) found the percentage of males to increase in small rodents when densities are high, while females predominate during the low phase. Other cases of an increased male fraction with increased density include white-tailed deer (*Odocoileus virginianus*) (McCullough 1979) and northern elephant seal (*Mirounga angustirostris*) (Le Boeuf and Briggs 1977). Individuals of voles and red grouse (*Lagopus lagopus scotica*) are more aggressive at high than low population densities, with red grouse having larger kin groups evolving during the increasing phase of a cycle (e.g. Boonstra and Krebs 1979; Matthiopoulos et al. 2003; Piertney et al. 2008).

When evaluating evidence for or against selection regulation it is essential to realise that selection regulation is the complete response of the population dynamic growth rate to natural selection. Genetic evolution is one potential response. Others include changes in maternal effects and social behaviour, long-term selected phenotypic plasticity in physiological and behavioural traits allowing individuals to respond directly to the cyclic change in the selection pressure, and epigenetic changes. Cultural inheritance is another factor, where most offspring may balance their quality/quantity investment in their offspring following the balance of their parents, with fewer offspring choosing another balance and thus maintaining the cultural heritable variance of the population.

As it is the joint selection response across these factors and more that generates the change in population dynamic growth, we cannot exclude selection regulation just because one component—like e.g. the genetic variance—is insufficient to account for the observed changes. It is like density regulation, where we do not exclude potential regulation just because we have not yet observed the underlying mechanistic details.

While it is impossible to exclude density regulation and selection regulation *a priori*, there are plenty of studies that estimate the existence and force of density regulation from statistical analyses of timeseries of abundance data (e.g. Turchin and Taylor 1992; Sibly

et al. 2005; Knape and de Valpine 2012). I aim to estimate not only the potential presence of density regulation but also of selection regulation as it is possible to distinguish between the two regulating forces statistically when we analyse timeseries of abundance estimates. This is possible because density regulation determines the growth rate as a monotonically declining function of density, while population dynamic feedback selection accelerates and decelerates the growth rate as a function of the density frequency dependent selection. The two regulations are thus shaping the dynamics in different ways, allowing us to estimate the two types of regulation when population dynamic models are fitted to timeseries of abundance estimates. I use this ability in this first large-scale analysis that estimates the presence and strength of density and selection regulation across almost four thousand populations of birds and mammals. This should show if selection regulation is weak, or whether it is so widespread and strong that we should include it in base-case population dynamic modelling.

2 Method

2.1 Data

To estimate density and selection regulation, I fitted population dynamic models to timeseries of abundance estimates. These were obtained from the Living Planet Index (LPI 2022), the North American Breeding Bird Survey (BBS; Sauer et al. 2017), the PanEuropean Common Bird Monitoring Scheme (EU; PECBMS 2022), the Netwerk Ecologische Monitoring (NET; Sovon 2022), the Swiss Breeding Bird Index (SWI; Knaus et al. 2022), the British Trust for Ornithology (BTO 2022), the Danish Ornithological Society (DOF 2022), and Svensk Fågeltaxering (SWE; SFT 2022).

Having different origin and scales of observation, the timeseries of especially the LPI are of varying quality. Thus, I used only timeseries with more than 10 abundance estimates over at least a 15-year period, resulting in 3,369 timeseries analysed for birds and 483 for mammals, with timeseries scaled for a geometric mean of unity. To avoid confounding effects, models were used for further analysis only if the mean of the residuals were not significantly different from zero ($p < 0.05$ student't), there were no significant autocorrelation in the residuals (lag 1 and 2), no significant correlation between the residuals and the model, and the model explained at least 50% of the variance.

I selected a subset of high-quality data that I analysed separately as a control. Most of the bird timeseries are standardised indices from point-counts, generated from indices for individual observers on individual routes with a given number of geographically fixed point-counts that are counted in the same way at the same time each year. The calculation of these indices is very standardised, correcting for observer and severe weather. Given a sufficient number of routes, these timeseries are of high quality.

A potential issue with bird indices is that their geographical coverage may not necessarily reflect individual populations. Population dynamics over large areas are often spatially synchronised (e.g. Ranta et al. 1995; Paradis et al. 1999; Liebhold et al. 2004), and to account for this I restricted my control timeseries to the population dynamics delineated indices (PDDIs) that Witting (2023b) compiled from the North American Breeding Bird Survey (Sauer et al. 2017). These are calculated from more than six million observations from USA and southern Canada, providing yearly abundance estimates for 51 years. Starting from indices that cover a $15x7$ longitudinal/latitudinal grid of the whole area, neighbouring indices with synchronised dynamics were lumped into larger areas, estimating 462 populations with different dynamics (Witting 2023b). The different PDDIs of a species are geographically separated at boundaries where the spatially synchronised dynamics desynchronise.

2.2 Population models

I incorporated the species-specific age structured demography into my models to scale them to the appropriate biological timescale, and account for the associated inherent delays in the dynamics. As the age structured demography cannot usually be estimated from timeseries, I obtained the equilibrium demographic parameters of all species from Witting (2024). Keeping these parameters fixed for each species, I estimated only the two regulation parameters and a few initial conditions from the abundance data. I used the equilibrium age structure as the initial age-distribution and, when necessary, I rescaled the yearly parameters for 3, 6, or 12 time-steps per year keeping the projection timesteps shorter than the age of maturity.

I developed exponential, hyperexponential, density regulated, and selection regulated models for each species. I found the best-fitting-hypothesis by the Akaike information criterion (AIC, Akaike 1973) to trade-off the number of parameters (from 2 to 5) against the likelihood of each model. This allowed me to estimate the relative probability of models with (hyperex-

ponential & selection regulated) and without (exponential & density regulated) selection.

As the AIC chose selection-based models most often (see result section), I ran a second AIC model-selection to estimate the best selection regulated models for all populations. In addition to a stable equilibrium, this second selection included models with a linear trend in equilibrium density. This allowed me to quantify not only the relative strengths of regulation by density and selection, but to estimate also if population trends are indicators of underlying changes in the external environment (assuming that a change in equilibrium reflects improved or deteriorating external factors).

I made regulation by density and selection operate on the birth rate ($m = \tilde{m}/m^*$) and age of reproductive maturity ($a_m = \tilde{a}_m/a_m^*$) by changes in relative parameters ($\tilde{m}$ and $\tilde{a}_m$) that were set to unity at population dynamic equilibrium (m^* and a_m^*). As I fitted the 1+ component of the population to the abundance data, the estimated regulation includes regulation on offspring survival. Hence, I covered regulation on the three life history parameters that are most sensitive to density dependent changes, allowing for regulation on a_m for an extended analysis of the PDDI timeseries only.

The Supplementary Appendix describes the selected regulated model, with essential differences between the four population models described below.

Exponential growth. This model has constant life history parameters, with the relative birth rate ($\tilde{m}$) and the initial abundance (n_t) estimated from data.

Hyperexponential growth. The age structured abundance ($n_{a,t}$) is the only initial condition of the exponential and density regulated models. A vector of competitive quality by age ($q_{a,t}$) is an extra initial condition in the selection models. This vector evolves with time, with selection for offspring of increased quality when the abundance is above the equilibrium abundance, and selection for a decline in quality when the abundance is below the equilibrium.

The age structured quality defines the age structured relative birth rate

$$\tilde{m}_{a,t} = 1/q_{a,t} \tag{1}$$

and relative reproductive maturity (when included for PDDI timeseries)

$$\tilde{a}_{m,a,t} = q_{a,t} \tag{2}$$

with $q^* = 1$ for all a representing the equilibrium with no growth.

Following the logic of the secondary theorem of natural selection (Robertson 1968; Taylor 1996), the selection induced change in competitive quality—and thus also in reproduction and reproductive age—is

$$q_{0,t} = q_t e^{-\gamma_\iota} \tag{3}$$

with average offspring quality (q_0) being a product between the average quality of the mature component

$$q_t = \frac{\sum_{a|a_{m,a,t}\leq a} q_{a,t} n_{a,t}}{\sum_{a|a_{m,a,t}\leq a} n_{a,t}} \tag{4}$$

and a selection response $e^{-\gamma_\iota}$, where

$$\gamma_\iota = -\sigma \, \partial r_i / \partial \ln q_i|_{q_i=q} \tag{5}$$

is the product between the selection gradient ($\partial r_i/\partial \ln q_i|_{q_i=q}$) across variants ($i$) and the response ($\sigma \geq 0$) of the population per unit selection, with σ reducing to the additive genetic variance for genetic evolution.

When there is no interactive competition and all individuals have equal access to resources, the intra-population variation in the growth rate of a discrete model is $r_i \propto -\ln q_i$ from eqn 1, with a selection gradient of $\partial r_i/\partial \ln q_i|_{q_i=q} = -1$ with $\gamma_\iota = \sigma > 0$. This is the limit case of hyperexponential growth at zero population density. Yet, I allowed for positive and negative γ_ι values to capture constantly accelerating ($\gamma_\iota > 0$) and decelerating ($\gamma_\iota < 0$) growth rates ($\gamma_\iota = 0$ is exponential growth). As the selection gradient on the per-generation growth rate is $-\partial r_i/\partial \ln q_i|_{q_i=q}$, the acceleration/deceleration of the growth rate is

$$\dot{r} = dr/dt = \gamma_\iota \tag{6}$$

The intra-population variation and the resulting population response of eqns 5 and 6 represent the underlying natural selection. Yet, it is not necessary to include this modelling of the intra-population variation into the population dynamic equations because the latter operates from the average response that is captured by eqns 3 and 4.

The hyperexponential model is structurally more complex than the exponential, but it has a only single parameter (γ_ι) and two initial conditions (n_t & q_t) to estimate from data.

Density regulated growth. I use the Pella and Tomlinson (1969) formulation

$$\tilde{m} = 1 + [\hat{m} - 1][1 - (n/n^*)^\gamma] \tag{7}$$

that has three parameters (maximum relative birth rate $\hat{m}$; density regulation γ; equilibrium abundance n^*) and one initial condition (n_t) to estimate from data.

Selection regulated dynamics. The selection regulated model includes density regulation

$$\begin{aligned} m_t &= m^* \tilde{m}_t (n^*/n_t)^\gamma \\ a_{m,t} &= a^*_m \tilde{a}_{m,t} (n_t/n^*)^\gamma \end{aligned} \tag{8}$$

as log-linear deviations from the equilibrium life history, with density regulation on a_m occuring only with a_m selection in the extended PDDI analysis.

The changes in competitive quality from the population dynamic feedback selection of density dependent interactive competition, was derived by Witting (1997, 2000) as

$$q_{0,t} = q_t (n_t/n^*)^{\gamma_\iota} \tag{9}$$

with the selection induced acceleration/deceleration of the growth rate

$$\dot{r} = \gamma_\iota \ln(n^*/n_t) \tag{10}$$

being a log-linear function of the density dependent ecology.

The selection behind eqns 9 and 10 is based on the biased resource access from the density frequency dependent interactive competition. The explicit modelling of the selection requires equations that account for the intra-population variation in competitive quality and resource access (Witting 1997, 2000). This produces the population level response of eqn 9 that is incorporated directly into the population dynamic equations.

The dynamics of population dynamic feedback selection is cyclic. Thus, I calculated the cycle period (T, in generations) and damping ratio (ζ) to characterise the dynamics. The damping ratio is zero for a stable cycle, increasing to unity for the monotonic return of density regulated growth. I calculated the damping ratio

$$\zeta = \frac{1}{\sqrt{1 + 4\pi^2/\delta^2}} \tag{11}$$

by the logarithmic decrement $\delta = \ln(n_{p,1}/n_{p,2})$ of the two successive abundance peaks ($n_{p,1}$ and $n_{p,2}$) that follow from an equilibrium population that is initiated with a positive growth rate where $q_{a,t} = 2q^*/3$. The estimated period (T) is the number of generations between these two abundance peaks.

When the γ_ι/γ-ratio increase above one the dynamics become unstable with amplitudes that increase over time instead of dampening out. In these cases, I reverted $n_{p,1}$ and $n_{p,2}$ in the estimate of $\delta = \ln(n_{p,2}/n_{p,1})$ and multiplied the ratio by minus one, so that negative ζ values refer to exploding cycles, with the rate of explosion increasing as ζ declines from zero to minus one.

The selection regulated model has three parameters (γ, γ_ι, & n^*) and two initial conditions (n_t & q_t) to estimate from data.

2.3 Model fitting & model selection

I used the likelihood (L) maximum to estimate the parameters of all models given log normally distributed abundance data

$$\ln L = -\sum_t \frac{[\ln(\tilde{n}_t/n_t)]^2}{2cv_t^2} + \ln cv_t \tag{12}$$

where $\tilde{n}_t$ is the 1+ index estimate in year t, n_t the corresponding model estimate, and $cv_t = \sqrt{\tilde{cv}_t^2 + cv^2}$ with $\tilde{cv}_t$ being the coefficient of variation of the index estimate, and cv additional variance that is not captured by the data. The latter is estimated by the likelihood fitting, capturing random variation in the dynamics of the population and variation in the population's availability to the yearly census.

I projected each model for 100,000 random parameter sets, applying a Quasi-Newtonian minimiser to the 100 best fits. Each of these minimisers located a local likelihood maximum, with the global maximum being the maximum across the local maxima. To avoid fitting fluctuating or chaotic dynamics to between-year variation in uncertain abundance estimates, I placed an upper limit of 1.5 on the estimates of γ and γ_ι.

The global maximum likelihood was converted to AIC [$\alpha = 2(k - \ln L)$, k nr. of model parameters] to select the best model for each species. I calculated the fraction of the AIC selected models that included selection, and the distribution of the probability ratio $p(s/d) = e^{(\alpha_s - \alpha_n)/2}$ of selection (s) versus non-selection models (d), with the s and d models being hyperexponential versus exponential, or density regulated versus selection regulated, depending upon the best AIC-fitting model.

I allowed one year of catastrophic survival for ten populations with a crash in abundance, and for seven large whale populations I subtracted annual catches from the dynamics following Witting (2013; data from https://iwc.int).

3 Results

I analysed 3,369 and 483 timeseries for 900 and 208 species of birds and mammals, with population models for 2,058 bird and 290 mammal populations passing the minimum fitting criterion during the first round of AIC model selection.

For the 2,348 timeseries with satisfactory models, the AIC selection chose selection-based models in 79% of the cases (79% for birds & 79% for mammals), with the selection-based models being 780 (se:1.3) times more

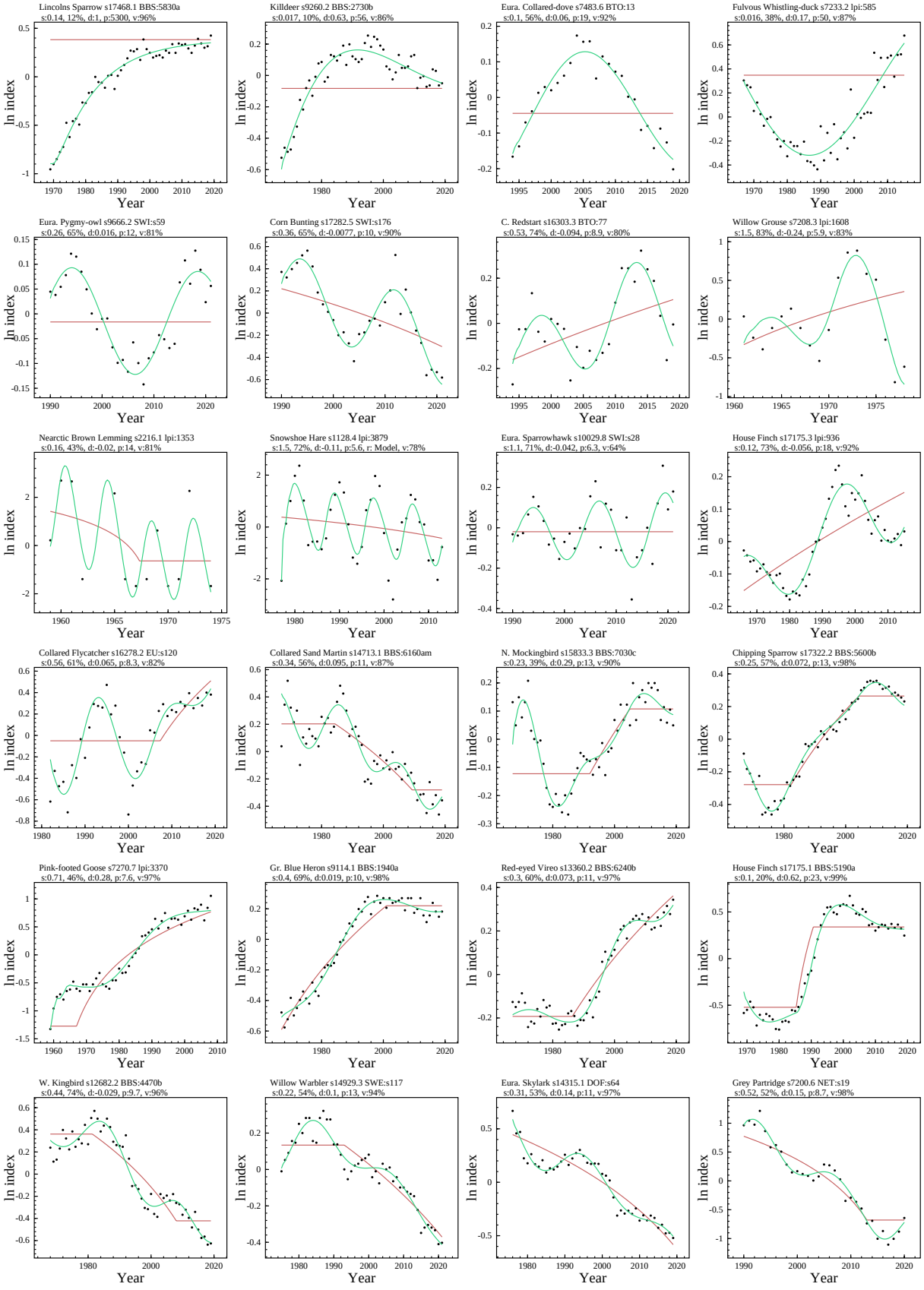

Figure 1: Examples of selection-regulated models fitted to population dynamic timeseries. Dots are index series of abundance, red lines the estimated equilibria, and green curves the model projections. Headings: name; id. nr; data reference; s:γ_ι & $\gamma_\iota/(\gamma_\iota+\gamma)$ in %; d:damping ratio; p:period in generations; v:explained variance in %.

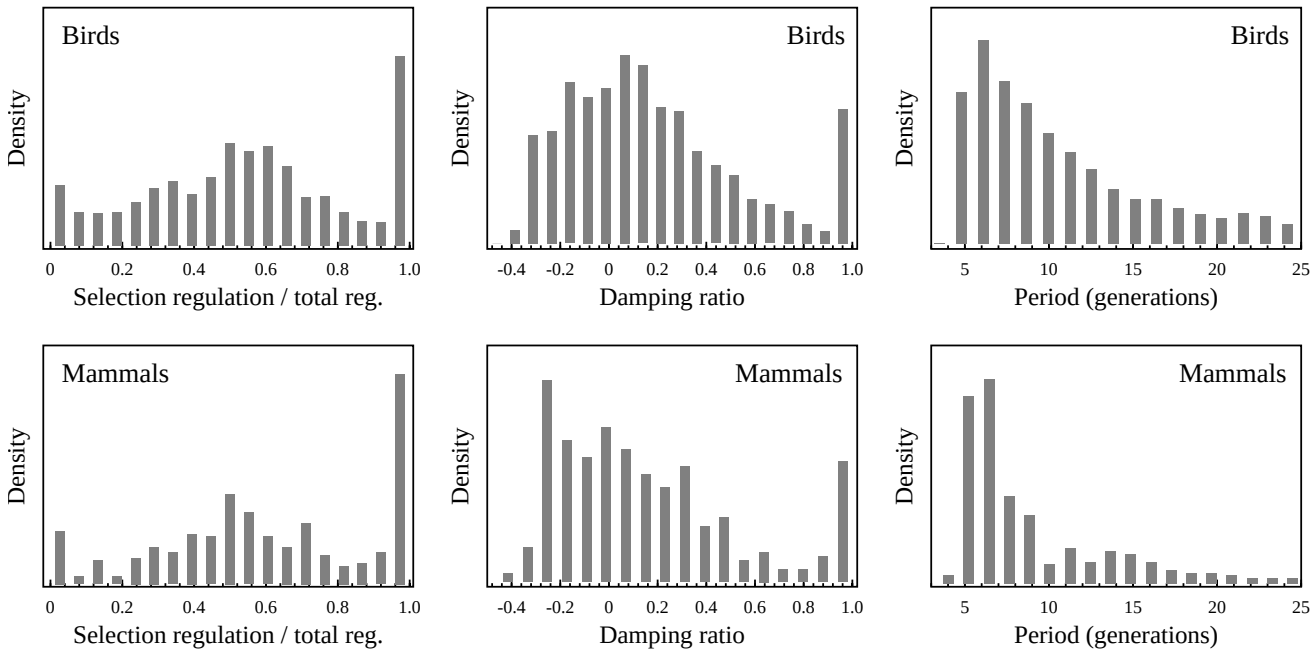

Figure 2: Distributions of the strength of selection regulation [divided by total regulation; $\gamma_\iota/(\gamma_\iota+\gamma)$], the damping ratio, and population period of the final AIC selected models for 2,480 bird and 321 mammal populations.

probable on average (geometric mean) than population dynamic models with no selection (based on relative AIC). The AIC selection chose selection regulated models in 43% of the cases, followed by 35% hyperexponential, 14% exponential, and 7.6% density regulated models.

Selection is even more pronounced in the PDDI control timeseries. Here, the AIC included selection in 92% of 267 chosen models, with selection-based models being 150,000 (se:2) times more probable on average than non-selection models. The AIC selection chose selection regulated model in 69% of the cases, followed by 23% hyperexponential models, 4.9% exponential, and 3.4% density regulated models.

With selection regulation covering all models (exponential when $\gamma = \gamma_\iota = 0$; hyperexponential when $\gamma = 0$ & $\gamma_\iota \neq 0$; density regulated when $\gamma > 0$ & $\gamma_\iota = 0$), I use the second AIC selection of selection regulated models with and without a change in equilibrium to describe the dynamics. This resulted in 2,801 accepted models (2,480 for birds; 321 for mammals) that explained 80% of the variance in the data, on average. 24 of the models are plotted in Fig. 1, with the Supplementary Information showing all accepted models.

The estimated median selection regulation (γ_ι) is 0.36 (se:0.01) for birds and 0.72 (se:0.032) for mammals, with median density regulation (γ) being 0.31 (se:0.0088) for birds and 0.31 (se:0.028) for mammals. The left plots in Fig. 2 show the distributions of the strength of selection regulation relative to total regulation [i.e., $\gamma_\iota/(\gamma+\gamma_\iota)$] across all timeseries with accepted selection regulated models. With median estimates of 0.55 (se:0.0058) for birds and 0.58 (se:0.017) for mammals, selection regulation is equally or more important than density regulation in most populations, with median regulation ratios (γ_ι/γ) of 1.2 (se:0.11) and 1.4 (se:0.37). These results resemble those of the PDDI controls, where relative selection regulation [$\gamma_\iota/(\gamma+\gamma_\iota)$] is 0.53 (se:0.012) at the median across 399 selection regulated models. Allowing for regulation on reproductive maturity among the PDDI controls, 47% of 408 accepted selection regulated models were AIC-selected with regulation on both the reproductive rate and age of maturity, with a median relative [$\gamma_\iota/(\gamma+\gamma_\iota)$] selection regulation of 0.61 (se:0.019) across all models.

The distributions of regulation estimates cover the range from almost pure selection regulation to almost pure density regulation. Only 7.3% of the bird and 6.5% of the mammal populations have selection regulation below 10% of total regulation by density and selection. These results cannot support the hypothesis that natural populations of birds and mammals are predominantly density regulated.

Where density regulated growth returns monotoni-

cally to the carrying capacity with a damping ratio around unity (like top left plot in Fig. 1), selection regulated populations have damped to stable population cycles (Fig. 1), with damping ratios that decline to zero for stable cycles. Some populations may even have exploding cycles with negative damping ratios during smaller time periods, although timeseries with negative damping ratio estimates may reflect uncertainty in our estimation of regulation.

The middle plots in Fig. 2 show the distributions of the estimated damping ratios. With median damping ratios around 0.12 (se:0.0071) and 0.062 (se:0.021) the population dynamics of birds and mammals is best characterised as strongly cyclic. 83% of the bird populations, and 85% of the mammals, have damping ratios that are smaller than 0.5. Only 7.3% of the bird populations, and 7.8% of mammals, have strongly damped density regulation like growth with damping ratios above 0.9.

The right plots in Fig. 2 show the distributions of the periods of the population cycles. Only 3% of the estimated periods are shorter than five generations. The distributions have long tails toward long periods, and they peak in the lower range with 46% of all birds, and 62% of all mammals, having periods below 10 generation. Median estimates are 11 (se:86) generations for birds and 7.9 (se:180) for mammals, and the period increases with stronger damping. The median period increases from 8.3 (se:0.99) and 7.2 (se:0.85) generations for birds and mammals with stable dynamics (damping ratios around zero), to 28 (se:9.5) and 15 (se:1.8) for damping ratios around 0.8.

Where density regulated populations tend to decline only if the environment deteriorates with a declining equilibrium abundance, selection regulated populations tend to decline about 50% of the time when the equilibrium is stable, declining, or increasing (Fig. 1, second line). Across the AIC chosen selection regulated models, the equilibrium abundancies increase for 30% and 21% of the bird and mammal populations and decline for 29% and 14%. For intervals where the estimated trajectories are either declining or increasing, 76% of the population dynamic declines were not associated with an estimated decline in the equilibrium abundance, and that 77% of the population dynamic increases were not associated with an equilibrium increase. In fact, 23% of the population declines had increasing equilibria, and 27% of the population increases had declining equilibria.

4 Discussion

As it is impossible to exclude both density regulation and selection regulation *a priori*, I estimated the two regulating forces statistically from timeseries of abundance estimates in birds and mammals. With AIC model-selection choosing selection-based models for 79% to 92% of the analysed timeseries, and median selection regulation being 1.2 (se:0.11) times stronger than density regulation, selection regulation is an important population dynamic component. Pure density regulation with damping ratios around unity is the exception rather than the rule and unsuited as base-case regulation for birds and mammals.

With selection regulation included we have a more elaborate single-species model that describes a broad range of the observed population dynamic trajectories (Fig. 1). These are cyclic with median damping ratios around 0.12 (se:0.0071) and 0.062 (se:0.021) for birds and mammals respectively, and population dynamic periods that increase with increased damping, with medians around 8.3 (se:0.99) and 7.2 (se:0.85) generations for stable cycles with damping ratios around zero.

These results are statistical estimates given the density regulated and selection regulated models, and they do not exclude other potential drivers. Yet, my statistical analyses accounted for other factors by including random environmental variation into estimates of the additional variance in the timeseries of abundance estimates, and I used linear trends in the equilibrium abundance to capture directional changes in extrinsic factors like habitats, resources, and predators. The statistical estimates do not account for secondary effects from e.g. phase related changes in predation mortality.

Apart from the observed similarity between model predictions and data, my analysis provides by itself no direct evidence on the underlying density and selection response in natural populations. Yet, empirical studies on population dynamic cycles have already documented the selection response extensively, with selection regulation resolving paradoxes between non-selection theory and observed population dynamic cycles.

We saw in the introduction how selection regulation predicts the widespread—and otherwise unexplained—phase related changes in a variety of life history traits for species with cyclic population dynamics. And with the estimated selection regulated dynamics generating damped phase forgetting cycles, low amplitude cycles are not a problem because the cyclic dynamics of selection regulation do not depend on high-density amplitudes for the build-up of predators, pathogens, or other detrimental factors. Selection regulation acceler-

ates and decelerates population growth in smaller steps per generation, and there is thus also no longer an issue with a low reproductive rate during the low phase where density regulation is relaxed.

The observed phase related changes in the life histories of cyclic populations cannot merely be secondary effects with no relation to the underlying cause of the cycles. This is because there will be no cycle in abundance unless there is a cycle in at least one life history parameter. The life history cycles are ultimately predicted by population dynamic feedback selection, and they are the proximate cause of the cyclic dynamics that maintains the cyclic selection for their continued, or damped, existence.

There is no reason to expect that the statistical support for selection regulation is an artefact of rejecting an unrealistically simple density regulated model. This is because selection regulation could, at least in principle, operate as density regulation resulting in an equally inflexible model, despite of the increased complexity imposed by selection. It is only because regulation by density and selection operates structurally differently on the dynamics that we can distinguish between the two components statistically in timeseries of abundance estimates. And AIC model-selection is only choosing selection regulated models over density regulated models because the increased dynamic flexibility comes at a low additional parameter cost. We can conclude that the population dynamics of birds and mammals support the population regulation structure of natural selection.

Delayed density regulated models have a similar statistical advantage, but they do not evaluate explicit biological hypotheses. A delayed regulation from explicitly identified inter-specific interactions should instead use a mechanistic model that includes the age structured delays of the life histories of the interacting species. This requires additional parameters, and inter-specific models are typically less parsimonious than selection regulated models (which have the same number of parameters as density regulated models, but one extra initial condition).

Population models with timestep specific environmental perturbations can always generate perfect fits between theoretical population trajectories and data. But this requires a unique perturbation to fit for each timestep in the timeseries, making them even less statistically supported. In the end, when constructing a dynamic model for a population, the parsimonious way is to analyse if the population regulation of the population will explain the dynamics of the population.

A partial decoupling between the extrinsic environment and population growth is one of the more intriguing consequences of selection regulation. Traditional density regulation thinking implies that we need a change in the extrinsic environment before the direction of population growth will change. This leads to the concept of indicators, where the population dynamic behaviour of indicator species are supposed to reflect the underlying state of the environment (e.g. ASTI 2016; LPI 2022; PECBMS 2022; CSI 2023). While environmental changes may change the growth direction of selection regulated populations, the direction of growth may also change in the absence of environmental changes. In other words, the growth of populations are not necessarily indicators of the environment, with about 75% of the estimated population declines in this study containing no signal of a deteriorating environment.

Another interesting consequence relates to the abundance of animals, which is left almost unexplained by traditional non-selection population dynamic theory (May 2020). This contrasts to population dynamic feedback selection that explains inter-specific abundance variation as a function of the naturally selected body mass with superimposed inter-specific competition (Witting 2023a). The density frequency dependent feedback selection of interactive competition is an essential factor for our understanding of the life histories, population dynamics, and abundancies of natural populations.

Acknowledgements

I thank reviewers for comments and all who collect and publish population dynamic data. The estimated population models are available for online simulations at https://mrLife.org.

Supplementary Information

si-appendix Model appendix

si-plot Population plots

References

Agashe D. (2009). The stabilizing effect of intraspecific genetic variation on population dynamics in novel and ancestral habitats. Am. Nat. 174:255–267.

Akaike H. (1973). Information theory as an extension of the maximum likelihood principle. In: Petrov B. N. Csaki F. (eds). Second International Symposium on Information Theory: Akademiai Kiado, pp 267–281.

Andreassen H. P., Sundell J., Ecke F., Halle S., Haapakoski M., Henttonen H., Huitu O., Jacob J., Johnsen K., Koskela E., Luque-Larena J. J., Lecomte N., Leirs H., Marien J., Neby M., Ratti O., Sievert T., Singleton G. R., Cann J. v., Broecke B. V., Ylonen H. (2021). Population cycles and outbreaks of small rodents: ten essential questions we still need to solve. Oecologia 195:601–622.

ASTI (2016). Arctic Species Trend Index. CAFF, Akureyri.

Bell G. Gonzalez A. (2009). Evolutionary rescue can prevent extinction following enviromental change. Ecol. Lett. 12:942–948.

Berryman A. A. (1996). What causes population cycles of forest lepidoptera? Trends Ecol. Evol. 11:28–32.

Boonstra R. Krebs C. J. (1979). Viability of large- and small-sized adults in fluctuating vole populations. Ecology 60:567–573.

Brunner F. S., Deere J. A., Egas M., Eizaguirre C., Raeymaekers J. A. M. (2019). The diversity of eco-evolutionary dynamics: Comparing the feedbacks between ecology and evolution across scales. Funct. Ecol. 33:7–12.

BTO (2022). British Trust for Ornithology. Population trend graphs. https://www.bto.org.

Chitty D. (1960). Population processes in the voles and their relevance to general theory. Can. J. Zool. 38:99–113.

Coulson T., Macnulty D. R., Stahler D. R., Vonholdt B., Wayne R. K., Smith D. W. (2011). Modeling Effects of Environmental Change on Wolf Population Dynamics, Trait Evolution, and Life History. Science 334:1275–1278.

CSI (2023). Canadian Environmental Sustainability Indicators: Canadian Species Index. Environment and Climate Change Canada, Gatineau.

DOF (2022). Dansk Ornitologisk Forening. Punkttællinger. https://www.dof.dk.

Elton C. S. (1924). Periodic fluctuations in number of animals: their causes and effects. Brit. J. Exp. Biolo. 2:119–163.

Fisher R. A. (1930). The genetical theory of natural selection. Clarendon, Oxford.

Ginzburg L. R. (1998). Inertial growth. Population dynamics based on maternal effects. In: Mousseau T. A. Fox C. W. (eds). Maternal effects as adaptations: Oxford University Press, New York, pp 42–53.

Gomulkiewicz R. Holt R. D. (1995). When does evolution by natural selection prevent extinction? Evolution 49:201–207.

Halley J. M., Vokou D., Pappas G., Sainis I. (2021). SARS-CoV-2 mutational cascades and the risk of hyper-exponential growth. Microbial Pathigenesis 161:https://doi.org/10.1016/j.micpath.2021.105237.

Hansen T. F., Stenseth N. C., Henttonen H., Tast J. (1999). Interspecific and intraspecific competition as causes of direct and delayed density dependence in a fluctuating vole population. Proc. Nat. Acad. Sci. USA 96:986–991.

Hodges K. E., Stefan C. I., Gillis E. A. (1999). Does body condition affect fecundity in a cyclic population of snowshoe hares? Can. J. Zool. 77:1–6.

Hörnfeldt B. (1994). Delayed density dependence as a determinant of vole cycles. Ecology 73:791–806.

Jenkins G. P., Coleman R. A., Barrow J. S., Morrongiello J. R. (2022). Environmental drivers of fish population dynamics in an estuarine ecosystem of south-eastern Australia. Fish. Manag. Ecol. 29:693–707.

Kaitala V., Ranta E., Lindstrom J. (1996). Cyclic population dynamics and random perturbations. J. Anim. Ecol. 65:249–251.

Keith L. B. (1963). Wildlife's ten year cycle. University of Wisconsin Press, Madison.

Knape J. deValpine P. (2012). Are patterns of density dependence in the Global Population Dynamic Database driven by uncertainty about population abundance? Ecol. Lett. 15:17–23.

Knaus P., Schmid H., Strebel N., Sattler T. (2022). The State of Birds in Switzerland 2022 online. http://www.vogelwarte.ch.

Koenig W. D. (2002). Global patterns of environmental synchrony and the Moran effect. Ecography 25:283–288.

Le Boeuf B. J. Briggs K. T. (1977). The cost of living in a seal harem. Mammalia 41:167–195.

Lidicker W. Z. Ostfeld R. S. (1991). Extra-large body size in California voles: Causes and fitness consequences. Oikos 61:108–121.

Liebhold A., Koenig W. D., Bjørnstad O. N. (2004). Spatial synchrony in population dynamics. Ann. Rev. Ecol. Evol. Syst. 35:467–490.

Liu R., Gourley S. A., DeAngelis D. L., Bryant J. P. (2013). A mathematical model of woody plant chemical defenses and snowshoe hare feeding behavior in boreal forests: the effect of age-dependent toxicity of twig segments. SIAM J. Appl. Math. 73:281–304.

LPI (2022). Living Planet Index database. www.livingplanetindex.org.

Martinez-Padilla J., Redpath S. M., Zeineddine M., Mougeot F. (2014). Insights into population ecology from long-term studies of red grouse *Lagopus lagopus scoticus*. J. Anim. Ecol. 83:85–98.

Matthiopoulos J., Moss R., Mougeot F., Lambin X., Redpath S. M. (2003). Territorial behaviour and population dynamics in red grouse *Lagopus lagopus scoticus*. II. Population models. J. Anim. Ecol. 72:1083–1096.

May R. M. (2020). What determines population density?. In: Dobson A., Holt R. D., Tilman D. (eds). Unsolved problems in ecology: Princeton University Press, Princeton, pp 67–75.

McCauley E., Nelson W., Nisbet R. (2008). Small-amplitude cycles emerge from stage-structured interac-

tions in daphniaalgal systems. Nature 455:1240–1243.
McCullough D. R. (1979). The George River Deer Herd: Population ecology of a k-selected species. Univ. Michigan Press, Ann Arbor.
McKane A. J. Newman T. J. (2005). Predator-prey cycles from resonant amplification of demographic stochasticity. Phys. Rev. Lett. 94:218102.
Murdoch W. W., Kendall B. E., Nisbet R. M., Briggs C. J., Mccauley E., Bolser R. (2002). Single-species models for many-species food webs. Nature 417:541–543.
Murdoch W. W. McCauley E. (1985). Three distinct types of dynamic behavior shown by a single planktonic system. Nature 316:628–630.
Myers J. H. (1990). Population cycles of western tent caterpillars: experimental introductions and synchrony of fluctuations. Ecology 71:986–995.
Myers J. H. (2018). Population cycles: generalities, exceptions and remaining mysteries. Proc. R. Soc. B. 285:20172841.
Naumov S. P., Gibet L. A., Shatalova S. (1969). Dynamics of sex ratio in respect to changes in numbers of mammals. Zh. Obshch. Biol. 30:673–680.
Norrdahl K. Korpimäki E. (2002). Changes in individual quality during a 3-year population cycle of voles. Oecologia 130:239–249.
Oli M. K. (2019). Population cycles in voles and lemmings: state of the science and future directions. Mamm. Rev. 49:226–239.
Paradis E., Baillie S. R., Sutherland W. J., Gregory R. D. (1999). Dispersal and spatial scale affect synchrony in spatial population dynamics. Ecol. Lett. 2:114–120.
Pavithran I. Sujith R. I. (2022). Extreme COVID-19 waves reveal hyperexponential growth and finite-time singularity. Chaos 32:041104.
PECBMS (2022). Pan-European Common Bird Monitoring Scheme. https://pecbms.info.
Pella J. Tomlinson P. (1969). A generalized stock production model. Trop. Tuna. Comm. Bull. 13:419–496.
Piertney S. B., Lambin X., Maccoll A. D. C., Lock K., Bacon P. J., Dallas J. F., Leckie F., Mougeot F., Racey P. A., Redpath S., Moss R. (2008). Temporal changes in kin structure through a population cycle in a territorial bird, the red grouse *Lagopus lagopus scoticus*. Mol. Ecol. 17:2544–2551.
Post E. Forchhammer M. C. (2002). Synchronization of animal population dynamics by large-scale climate. Nature 420:168–171.
Ranta E., Kaitala V., Lindstrom J., Linden H. (1995). Synchrony in population dynamics. Proc. R. Soc. Lond. B. 262:113–118.
Robertson A. (1968). The spectrum of genetic variation. In: Lewontin R. C. (ed). Population Biology and Evolution: Syracuse University Press, New York, pp 5–16.
Saccheri I. Hanski I. (2006). Natural selection and population dynamics. Trends Ecol. Evol. 21:341–347.
Sauer J. R., Niven D. K., Hines J. E., Ziolkowski D. J., Pardieck K. L., Fallon J. E., Link W. A. (2017). The North American Breeding Bird Survey, Results and analysis 1996 – 2015. Version 2.07.2017. USGS Patuxent Wildlife Research Center, Laurel, Maryland, Available at www.mbr-pwrc.usgs.gov/bbs/bbs.html.
SFT (2022). Svensk Fågeltaxering. http://www.fageltaxering.lu.se.
Sibly R. M., Baker D., Denham M. C., Hone J., Pagel M. (2005). On the regulation of populations of mammals, birds, fish, and insects. Science 309:607–610.
Simchuk A. P., Ivashov A. V., Companiytsev V. A. (1999). Genetic patters as possible factors causing population cycles in oak leafroller moth, *Tortrix viridana* L. For. Ecol. Manage. 113:35–49.
Sinervo B., Svensson E., Comendant T. (2000). Density cycles and an offspring quantity and quality game driven by natural selection. Nature 406:985–988.
Sovon (2022). Netwerk Ecologische Monitoring, Sovon. Provincies & CBS. http://sovon.nl.
Stenseth N. C. (1981). On chitty's theory for fluctuating population: the importance of genetic polymorphism in the generation of regular density cycles. J. theor. Biol. 90:9–36.
Taylor P. D. (1996). The selection differential in quantitative genetics and ess models. Evolution 50:2106–2110.
Taylor R. A., White A., Sherratt J. (2013). How do variations in seasonality affect population cycles? Proc. R. Soc. Lond. B. https://doi.org/10.1098/rspb.2012.2714.
Thompson J. N. (1998). Rapid evolution as an ecological process. Trends Ecol. Evol. 13:329–332.
Turchin P. Taylor A. D. (1992). Complex dynamics in ecological time series. Ecology 73:289–305.
Turcotte M. M., Reznick D. N., Hare J. D. (2011). The impact of rapid evolution on population dynamics in the wild: experimental test of eco-evolutionary dynamics. Ecol. Lett. 14:1084–1092.
Tyson R., Haines S., Hodges K. (2010). Modelling the Canada lynx and snowshoe hare population cycle: the role of specialist predators. Theor. Ecol. 3:97–111.
Witting L. (1997). A general theory of evolution. By means of selection by density dependent competitive interactions. Peregrine Publisher, Århus, 330 pp, URL https://mrLife.org.
Witting L. (2000). Population cycles caused by selection by density dependent competitive interactions. Bull. Math. Biol. 62:1109–1136, https://doi.org/10.1006/bulm.2000.0200.
Witting L. (2002). From asexual to eusocial reproduction by multilevel selection by density dependent competitive interactions. Theor. Pop. Biol. 61:171–195, https://doi.org/10.1006/tpbi.2001.1561.
Witting L. (2013). Selection-delayed population dynamics in baleen whales and beyond. Pop. Ecol. 55:377–401, https://dx.doi.org/10.1007/s10144–013–0370–9.

Witting L. (2017). The natural selection of metabolism and mass selects lifeforms from viruses to multicellular animals. Ecol. Evol. 7:9098–9118, https://dx.doi.org/10.1002/ece3.3432.

Witting L. (2023a). On the natural selection of body mass allometries. Acta Oecol. 118:103889, https//dx.doi.org/10.1016/j.actao.2023.103889.

Witting L. (2023b). Population dynamic population delineation in North American birds. Preprint at bioRxiv https://dx.doi.org/10.1101/2023.08.29.555290.

Witting L. (2024). Population dynamic life history models of the birds and mammals of the world. Ecol. Info. 80:102492.

Wynne-Edwards V. (1959). The control of populatiob density through social behaviour: A hypothesis. Ibis 101:436–441.

Wynne-Edwards V. C. (1986). Evolution through group selection. Blackwell Scientific Publications, Oxford.

5 Model appendix

The age-structure of each model is determined from three species specific parameters obtained from Witting (2024). These are the age of reproductive maturity (first reproductive event) in years ($\tilde{a}_m$), the annual rate of reproduction at population dynamic equilibrium ($\tilde{m}^*$), and the reproductive period ($\tilde{t}_r$). These parameters were converted to the appropriate timescale, with $a_m = \tilde{a}_m/\Delta t$, $m^* = \tilde{m}^*\Delta t$, and $t_r = \tilde{t}_r/\Delta t$ with $\Delta t \ll \min(\tilde{a_m}, \tilde{t}_r)$ being the timestep of the simulation model in years. The survival of all 1+ age-classes was then calculated as $p = (t_r - 1)/t_r$, with age-class zero survival being $p_0 = 2/t_r m^* p^{a_m - 1}$.

With $x \gg a_m$ being the maximum lumped age-class, the number $n_{a,t}$ of individuals of age $0 < a < x$ at timestep t is

$$n_{a,t} = p_{a-1} n_{a-1,t-1} \tag{13}$$

and the number in age-class x

$$n_{x,t} = p_x n_{x,t-1} + p_{x-1} n_{x-1,t-1} \tag{14}$$

with $p_a = p_0$ for $a = 0$ and $p_a = p$ for $a \geq 1$. Let the number of individuals in each age-class relate to time just after each timestep transition, with offspring at t being produced by the $t-1$ individuals that survive to the $t-1 \rightarrow t$ transition, with the density dependent ecology being approximated by the average 1+ abundance of the two timesteps:

$$\hat{n}_t = 0.5 \sum_{a \geq 1} n_{a,t} + n_{a,t-1}. \tag{15}$$

Together with the quality-quantity trade-off, the competitive qualities of the individuals define their relative birth rate

$$\tilde{m}_{a,t} = 1/q_{a,t} \tag{16}$$

as well as their relative age of reproductive maturity

$$\tilde{a}_{m,a,t} = q_{a,t} \tag{17}$$

with the population dynamic equilibrium having $q^* = 1$ for all a. More generally $q_{a,t} = q_{a-1,t-1}$ and

$$q_{x,t} = \frac{q_{x,t-1} p_x n_{x,t-1} + q_{x-1,t-1} p_{x-1} n_{x-1,t-1}}{n_{x,t}} \tag{18}$$

assuming that there is no change in the quality of a cohort over time. The quality of offspring

$$q_{0,t} = \frac{\sum_{a|a_{m,a,t} \leq a} q_{a,t} n_{a,t}}{\sum_{a|a_{m,a,t} \leq a} n_{a,t}} \left(\frac{\hat{n}_t}{\hat{n}^*} \right)^{\gamma_\iota} \tag{19}$$

is the average quality of the mature component multiplied by the density dependent selection, with γ_ι being the selection response.

Density regulation

$$\begin{aligned} m_{a,t} &= m^* \tilde{m}_{a,t} (\hat{n}^*/\hat{n}_t)^\gamma \\ a_{m,a,t} &= a^*_m \tilde{a}_{m,a,t} (\hat{n}_t/\hat{n}^*)^\gamma \end{aligned} \tag{20}$$

is formulated as a log-linear deviation from the equilibrium life history, with γ being the strength of regulation, and the number of offspring in age-class zero being

$$n_{0,t} = 0.5 \sum_{a|a_{m,a,t} \leq a} m_{a,t} n_{a,t}. \tag{21}$$

The initial conditions of an iteration are the same quality across all individuals and the initial abundance with a stable age-structure

$$c_a = l_a / \sum_{a \geq 0} l_a \tag{22}$$

where $l_0 = 1$, $l_a = p_0\ p^{a-1}$ for $1 \leq a < x$, and $l_x = p_0\ p^{x-1}/(1-p)$.

The population dynamic behaviour of a discrete version of the selection-regulated model was described by Witting (1997, 2000b). This model has damped population cycles when $\gamma_\iota < \gamma$, neutrally stable cycles when $\gamma_\iota = \gamma$, and repelling cycles when $\gamma_\iota > \gamma$. The population period of the stable cycles increases from four to an infinite number of generations as the $\gamma_\iota = \gamma$ parameters decline from two to zero. For a given γ the period increases with a decline in γ_ι, i.e., with an increasingly damped cycle. When, for a stable cycle, $\gamma_\iota = \gamma$ increases from two to four, there is an extra period in

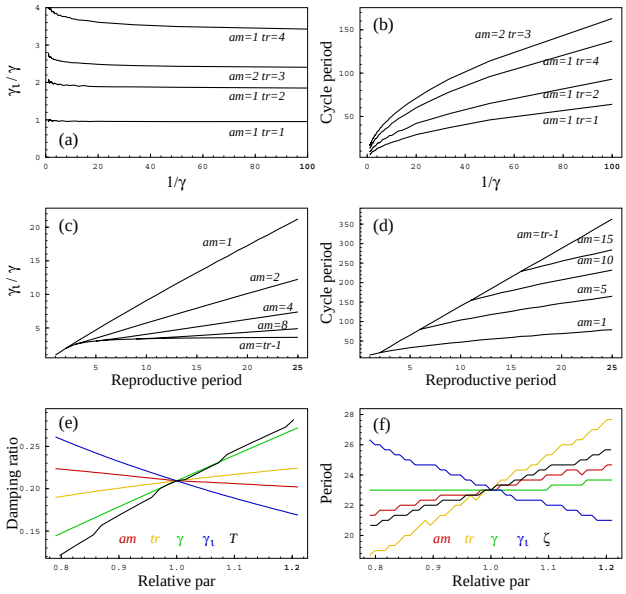

Figure 3: **Dynamic behaviour. Plot a to d:** The γ_ι/γ-ratio, and period (in years), of a stable population cycle ($\zeta = 0$) as a function of $1/\gamma$ (plot **a** and **b**) and the reproductive period (plot **c** and **d** for $\gamma = 0.2$), for different combinations of tm and tr. **Plot e and f:** The damping ratio (ζ) and population period (T) as a function of the parameters $x \in \{am, tr, \gamma, \gamma_\iota, \zeta, T\}$, relative ($x/\hat{x}$) to $\hat{x} \in \{am = 1, tr = 2.8, \gamma = 0.51, \gamma_\iota = 0.76, \zeta = 0.21, T = 23\}$. The dependence on T in plot **e**, and on ζ in plot **f**, is given by their responses to changes in γ_ι.

the amplitude of the population period, with the latter declining monotonically to two generations, with the dynamics becoming chaotic when $\gamma_\iota = \gamma$ increases beyond four.

The age-structured model with overlapping generations behave in a similar way, but the dynamics depend on the age of reproductive maturity (a_m) and the reproductive period [$t_r = 1/(1-p)$]. The age-structured model converges on the discrete model as $a_m \to 1$, $t_r \to 1$, and $p \to 0$. With no regulation on maturity, the period (T) of the stable population cycle remains a declining function of γ (Fig. 3b), with the slope/exponent (β) of the $\ln T \propto \beta \ln \gamma$ relation being -0.5 (estimated by linear regression). The cyclic dynamics become more and more stable with a decline in γ_ι, but the damping is also dependent on a_m and t_r. The stable cycle, e.g., has a γ_ι/γ ratio that increases beyond unity as a_m and t_r increase above unity (Fig. 3a and c). For any given combination of a_m and t_r, the stable cycle has a γ_ι/γ ratio that is almost constant (Fig. 3a).

For a given γ, the period of the stable population cycle increases almost linearly with an increase in a_m and t_r (Fig. 3d), with the period dependence on γ being somewhat elevated relative to the discrete model where $a_m = t_r = 1$ (Fig. 3b). Hence, for populations where γ is independent of a_m and t_r, we can expect an approximate linear relation between the population period T and life history periods like a_m and t_r.

When only one parameter is altered at the time, the period is almost invariant of γ (Fig. 3f). This reflects that the decline in period with an increase in γ for dynamics with a given damping ratio, is counterbalanced by the increase in period that is caused by the increased stability of the cycle, as the γ_ι/γ ratio—that defines the damping ratio—declines with the increase in γ. For single parameter perturbations, the damping ratio is usually most strongly dependent on γ and γ_ι, showing only a small increase with t_r and a small decline with an increase in a_m (Fig. 3e).